VOL. 18, NO. 6, MARCH 2023 ISSN 1819-6608
ARPN Journal of Engineering and Applied Sciences

www.arpnjournals.com

MAPPING AND PREDICTING OF WATER EROSION USING RUSLE IN THE MEDITERRANEAN CONTEXT: CASE OF EL KHARROUB WATERSHED (WESTERN RIF, NORTHERN MOROCCO)

Zakaria Ammari[1], El Mostafa Mili[1], Ali Essahlaoui[1], Mohammed El Hafyani[1], Narjisse Essahlaoui[1], M'hamed Boufala[2], Abdessalam Ouallali[3], Farida Berrad[4] and Habiba Aassoumi[5]

[1]Department of Geology, Faculty of Sciences, Moulay Ismail University, Laboratory of Geoengineering and Environment, Research Group "Water Sciences and Environment Engineering, Zitoune, Meknes BP, Morocco
[2]National Office of Electricity and Drinking Water, Water Branch, Fes, Morocco
[3]Faculty of Sciences and Techniques of Mohammedia, Process Engineering and Environment Laboratory, Hassan 2 University, Casablanca, Morocco
[4]Regional Directorate of Forestry and Fight against Desertification of Rif, (SEAP), Tetouan, Morocco
[5]Abdelmalek Essaadi University, Faculty of Sciences, Laboratory of Environmental Geology and Natural Resources, Cartography and Digital Technologies' Team, Mhannech II, Tetouan, B. P., Morocco
E-Mail: zakaria.ammari@edu.umi.ac.ma

ABSTRACT

Worldwide, soil erosion is one of the hazards posing a serious threat to soil and water resources, especially in the Mediterranean context. In Morocco, this phenomenon is a major problem in the natural territory, especially in the Rif Mountains in the north of the country, where fragile rocks dominate on steep slopes. Thus, this work aims to assess the soil erosion in the El Kharroub River watershed over the baseline period 2000-2020 and two future periods 2021-2030 and 2031-2050, using the Revised Universal Soil Loss Equation (RUSLE). For the future climate periods (2021-2030 and 2031-2050), precipitations were produced using a classical statistical downscaling model (SDSM). Over the current period, the results showed that the annual rainfall erosivity and the vegetation cover decreased from 2002 to 2020 by 34.3% and 28.6% respectively. The annual soil loss maps showed a decline of about 54.8% during the baseline period. The changes in rainfall and vegetation cover are largely due to climate changes effect and the deforestation/reforestation that the region has experienced, which subsequently leads to changes in soil erosion due to the important function of these two factors. Furthermore, projected scenarios revealed that the average annual erosivity could decrease to 268.4 and 267.1 for 2031-2050 and 2031-2050 scenarios compared with the current period. As a result, the average annual soil losses could decrease by 21.3 and 21.8% for the projected scenarios.

Keywords: soil erosion, El kharroub watershed, Morocco, RUSLE, downscaling model.

1. INTRODUCTION

Soil and water are very important natural resources, thanks to their contribution to agricultural production along with food security [1], [2]. According to the Food and agriculture organization [3], Soil is a vital resource for human life, as it serves many economic and ecological functions, it stores and filtrates drinking water, constitutes the natural medium for the growth of plants, and is the substrate for landscapes and forests. The fact that this natural body is the result of a long process of rock alteration with the influence of weather, topography and organisms, makes it different from original rock in consistency, texture and physicochemical characteristics. Because of its weak consistence, soil is very vulnerable and can be easily degraded. Soil degradation is the result of different processes such as erosion, salinization, acidification and nutrient depletion [4]. Soil degradation causes a threat to food security, it reduces yield, forces farmers to use more inputs and in extreme cases abandon their land and look for new and more fertile lands. Indeed, if soil is completely degraded, it is not impossible to remediate it. It is a nonrenewable resource considering the human lifetime scale.

Soil erosion induced by rainfall and runoff is known as water erosion, which constitutes a major factor in soil degradation and siltation of dams [4], [5]. This process causes multiple problems; when the topsoil containing organic matter is eroded, an important change in soil quality occurs and thereby reducing soil productivity [6]. Soil erosion has also negative effects on water resources and the biodiversity of rivers' ecosystems. For example, it affects the physicochemical parameters of water, local fish fauna, aquatic plants and other biotic life [7]. Sedimentation of transported materials is an offsite problem causing a decline in dams' storage capacity [8], thus the reduction of reservoirs' lifetime and electricity production. In fact, soil erosion is a natural phenomenon processed by several natural factors that are not easy to control involving climate change, topography, soil friability and vegetation cover. Rainfall drop splash is the most important factor triggering erosion [9]; in addition, the combined influence of rainfall amount and intensity has much greater impact on soil erosion than the impact of rainfall amount alone [10]. The onsite experiments of [11] found out that the variability in soil losses is due to differences in soil characteristics, microrelief, and slope occurred among the experimental plots. Despite erosion being a nature dependent phenomenon, it can be accelerated by anthropic activities that change land use and land cover. Guo *et al.,* 2019 [12] reported that the increase in converting forests, scrublands and grasslands to croplands aggravates soil erosion.

Soil erosion has been studied by qualitative and quantitative methods. Quantitative methods include the ^{137}Cs technique, erosion plots, dams' bathymetry, turbidity, SWAT, USLE model and it's modified (MUSLE) and revised (RUSLE) versions. For example, the ^{137}Cs method was used to quantify soil loss in [13], [14], [15]. Bathymetry and turbidity were used in northern Morocco by Moukhchane in 2001 [16]. Other researchers choose the MUSLE model for estimating sediment yield [17] or soil and water assessment tool (SWAT) [18], [19], and [20]. Nowadays, the USLE and RUSLE models is still the most widely quantitative models used to assess soil erosion throughout the world. Since the 1970s USLE model was published by Weishmeir and smith, 1978 [21] and it still popular and used by recent research [22] and [23]. The RUSLE model [24] remains the first one of the top most applied tools in the world as found in the global review highlighted by [25]. For example in Asia the model is used recently by [26],[27] and [28]. In Africa, many studies tend to assess water erosion with the aid of RUSLE model [29], [5], and [30]. In the Mediterranean environment [31], [32] and [33].

The RUSLE model can characterize areas with severe or extreme risk to define the priority of management. The rating of soil erosion is expressed by mass of soil eroded per unit area per unit of time. Under natural conditions, annual rates are of the order of 0.0045 t/ha for moderate relief areas and 0.45 t/ha for steep one. In comparison, rates from agricultural lands are in the range of 45-450 t/ha [4]. Nowadays, prediction of soil erosion has become possible using climate prediction models, and important for the decision makers to perform protection techniques in the future. For example, statistical downscaling model (SDSM) was used to predict climate and soil erosion in several works [9], [33], [34] and [35]. Given this context, the specific objectives were: i) assessment of soil erosion rate in the watershed for a basis period of 2000-2020 and for two future time periods 2021-2030 and 2031-2050; ii) analyze the variation of the annual rainfall and the vegetation cover to better quantify their contributions to the erosion risk.

2. METHODOLOGY

2.1 Study Area

El kharroub watershed covers an area of 182.06 Km², and itis in the North of Morocco at the boundary between Tetouan and Larache provinces (Figure-1). The climate is influenced by both the Mediterranean climate and the Atlantic proximity, it is known by moderate temperatures (18.3 °C) and high annual precipitations in the order of700mm. The topography changes greatly from east to west with mountains, hills and plains (Figure-1). The eastern part corresponding to its upstream shows higher altitudes, the maximum altitude is about 1058m at the Mountains of Numidiannappes. The western part corresponding to its downstream shows lower altitudes, the minimum altitude is around 41m. In terms of dominance of the altitude classes, the low altitude class (41-200m) that corresponds to the dominant class with a percentage of 40.8%.The study area comprises variant degrees of slope, with steep slopes (more than 15 degrees) in the north eastern part and flat terrain in the west.

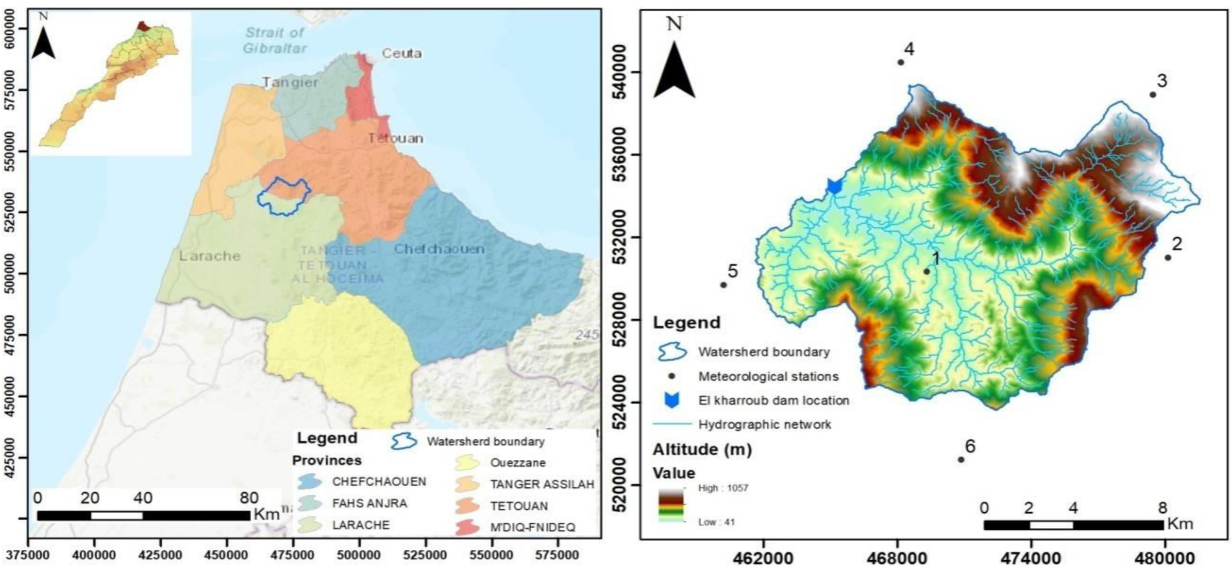

Figure-1. Geographical location of El Kharroub watershed.

2.2 Dataset and Processing

The RUSLE model helps to predict the average annual rate of soil loss (in t/ha/year) related to sheet or gully erosion by integrating five factors (Equation 1). The workflow (Figure-2) requires several sources of data: the digital terrain model (DEM), satellite images, climate data and soil maps. The DEM used is that of the Advanced Spaceborne Thermal Emission and Reflection Radiometer ASTER mission with a spatial resolution of 30m. While the satellite data were downloaded from USGS platform

ARPN Journal of Engineering and Applied Sciences

(https://earthexplorer.usgs.gov/), whose Landsat images were used for the first two dates ETM$^+$ for 2002 and OLI for 2014, while a sentinel image was used for the year 2020. For calculating soil loss by RUSLE, five factors are multiplied(Equation 1):

$$A = R \times K \times LS \times C \times P \quad (1)$$

Where: A is the soil loss rate (t/ha/year); R represents the rainfall erosivity factor (MJ.mm/ ha.h.an);K represents the soil erodibility factor(t.h/ha.MJ.mm);LS represents topographic factor; C represents land cover factor and P represents factor of the anti-erosion techniques.

R factor

This factor corresponds to the erosive power of rainwater. The more storms produce a high value of rain over a long period of time, the stronger the erosive power [36]. According to Wischmeier and Smith, 1978 [21], this factor (equation 2) is calculated using the kinetic energy of a storm (E) and the maximum rainfall intensity for 30 minutes (I_{30}):

$$R = E \times I_{30} \quad (2)$$

Because of the difficulty to get measurements of maximum rainfall intensity every 30 minutes, other researchers developed other formulas depending on the scale of record (daily, monthly or yearly). For our case, we used the formula of Renard and Freimund, 1994 [37] that utilize (equation 3) where yearly amounts of rainfall less than 850mm and (equation 4) for the opposite case:

$$\mathrm{R} = 0.0483 \times \mathrm{P}^{1.61} \quad (3)$$

$$\mathrm{R} = 587.8 - 1.219 \times \mathrm{P} + 0.004105 \times \mathrm{P}^2 \quad (4)$$

K factor

This factor represents a quantitative estimate of the sensitivity or resistance of a soil type to erosion. In general, if only soil characteristics are considered, soils with high silt and very fine sand content, low organic matter content, low structure and very low permeability will be the most sensitive to erosion [36]. To calculate K factor, Wischmeier and Smith, 1978[21] developed the following formula (Equation 5):

$$100K = 2{,}1 \times M^{1{,}14} \times 10^{-4} \times (12 - a) + 3{,}25 \times (b - 2) + 2{,}5 \times (c - 3) \quad (5)$$

Where: M =(%silt +very fine sand) x (100 - %clay), a = percentage of organic matter, b=soil structure code used in soil classification, c = profile permeability class.

LS factor

LS factor indicates the influence of the slope and its length on the rate of erosion. The steeper and longer the slope, the greater the risk of erosion occurs. For the calculation of this factor in our study, we used the formula developed by Mitasova *et al.*, 1996 [38]. This formula (Equation 6) uses flow accumulation; slope and DEM cell size as follows:

$$\mathrm{LS} = \left(\frac{\text{flow accumulation} \times \text{cell size}}{22.1}\right)^{0.6} \times \left(\frac{\mathrm{Sin(slope)} \times 0.01745}{0.09}\right)^{1.3} \quad (6)$$

C factor

This factor corresponds to the influence of the vegetation cover density on erosion. Vegetation cover plays an important role in protecting the soil it covers, as it reduces the impact of raindrops; it constitutes an obstacle to runoff and supports the soil structure. Recent studies used remote sensing to calculate C factor based on mathematical equations incorporating the Normalized Difference Vegetation Index (*NDVI*). This index is involved in the equation developed by Vander Knijff *et al.,* 1999[39] to calculate the C factor (Equation 7):

$$C = exp\left(-2 \times \frac{NDVI}{(1-NDVI)}\right) \quad (7)$$

Satellite images downloaded from the USGS have been used to construct the spatial distribution of *NDVI* in the El Kharroub watershed. *NDVI* is amonoband raster layer obtained by mathematical calculation integrating two bands red and near infrared (Equation 8):

$$NDVI = \frac{PIR-R}{PIR+R} \quad (8)$$

P factor

This factor describes soil conservation practices that reduce the erosive power of water by modifying the flow pattern or the slope. In general, a conservation practice is more effective when it protects the soil from mobilization caused by the impact of raindrops or when it causes deposition of eroded sediments close to the site where they originated. The practice near watershed downstream is less advantageous for soil conservation planning [36]. The most protective anti-erosion techniques used are contour cultivation, terrace cultivation, alternate strip cultivation, bench planting, stony cordons and anti-erosion benches. The P factor values are less than or equal to 1 depending on the technique used. In case, where none of these anti-erosion techniques is used, the P factor takes the value of 1.

VOL. 18, NO. 6, MARCH 2023 ISSN 1819-6608
ARPN Journal of Engineering and Applied Sciences

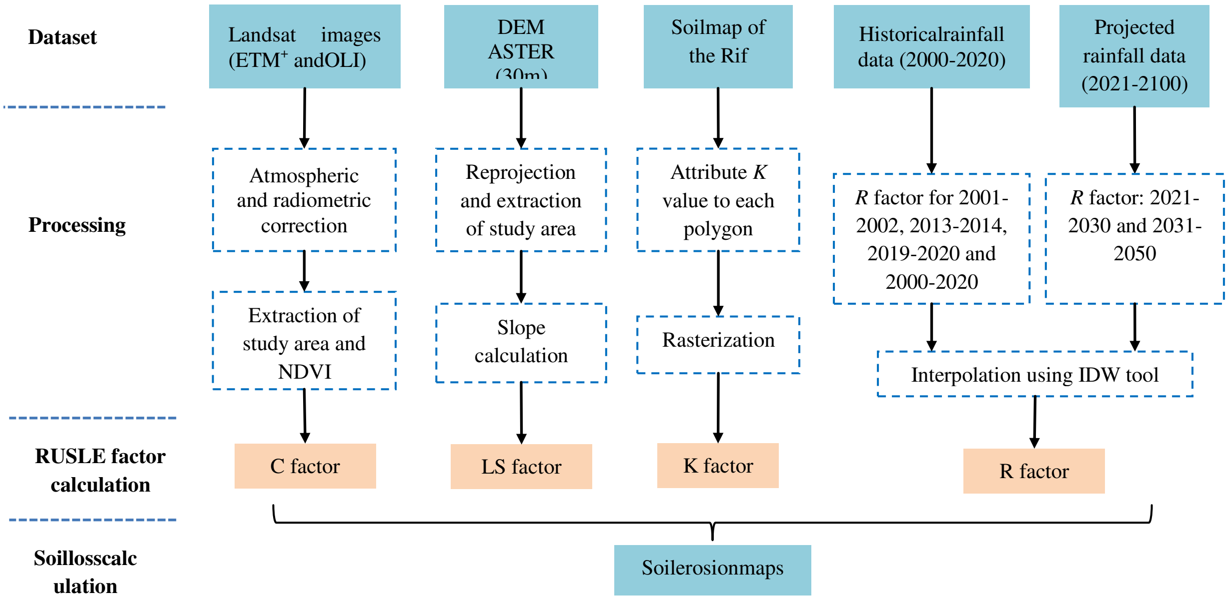

Figure-2. Flowchart of the adopted methodology.

3. RESULTS AND DISCUSSIONS

3.1 RUSLE Model

Climate Aggressiveness factor (R): In general, the results of *R* factor (Figure-3) show great values with high temporal variability. Over the baseline period, the minimum value of *R* factor (117 Mj.mm/ha/y) was obtained in station 5 for the period 2004-2005, while the maximum value (858.9 Mj.mm/ha/y) was found in station 2 for the year 2009-2010. The average annual rainfall erosivity is 308.4, 145.5,202.6 and 341.6 for 2001-2002, 2013-2014, 2019-2020 and 2000-2020 scenarios, respectively. In 2001-2002, the highest values up to 333.5 were obtained in the extreme north and northeastern parts of the watershed and small values starting with 291.5 were indicated in the south. The highest values in 2013-2014 were obtained in the northern and northwestern of the basin reaching 150, while the lowest values characterize the middle and southern sites. In the other hand, R factor of 2019-2020 is ranging from 198.5 to 213; highest values are shown in the northeastern extremity and lowest ones in the south and east.

In the predicted periods, the mean annual erosivity value is 268.5 and 267.1 for RCP 4.5 (2021-2030) and RCP 4.5 (2031-2050) scenarios, respectively. The spatial distribution is similar in the two predicted periods. It shows highest values in the northeastern parts and lowest values in the south sites. Compared with baseline period, the average rainfall erosivity will decrease by 21.39% and 21.81% for 2021-2030 and 2031-2050 scenarios, respectively.

ARPN Journal of Engineering and Applied Sciences

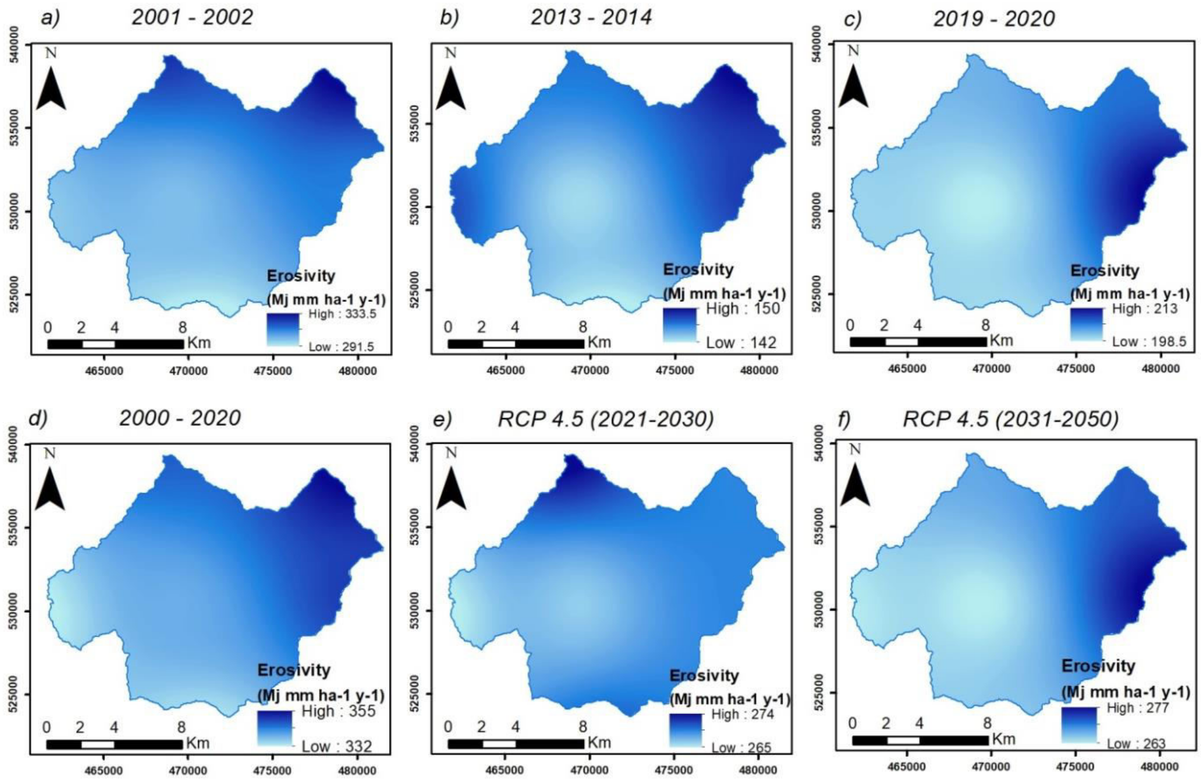

Figure-3. Spatial distribution of *R* factor for the different scenarios.

Soil erodibility factor K: The soil erodibility values were obtained from the regional directorate of water and forests and the fight against desertification. The *K* factor map (Figure-4.a) shows a mean value of 0.35. The map indicated the presence of five different soil types: low erodible soils with *K* value equal to 0.19 and are located downstream of the basin, close to the site of the dam, 2) soils with K value 0.21, located at the upstream of the watershed, 3) soils with *K* value of 0.24 at the southern and northern ends of the basin, 4) soils that have erodibility value of 0.41 located in the middle parts of the basin and around the south of the mainstream of El kharroub, and 5) finally soils that constitute the most erodible type, one part is located at the North of Oued El kharroub and the other part is located at the North-Eastern extremity of the basin.

Topographic factor LS: The topographic factor (Figure-4.b) ranges from 0.1 to 37.1 with a mean value of 4.3. The low values are found in the vicinity of Oued Kharroub, where the altitude is low, and the topography is flat. However, the higher values characterize the Numidian Sandstone Mountains with high altitudes of about 1050m (Figure-4.b) dominating the northeastern regions of the area.

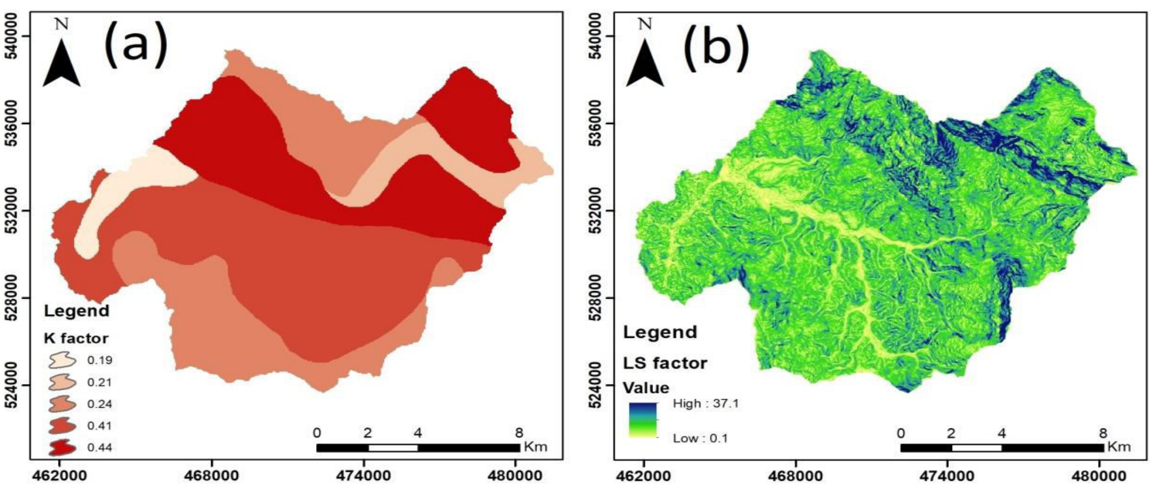

Figure-4. Spatial distribution of (a) *K* factor and (b) *LS* factor.

ARPN Journal of Engineering and Applied Sciences

Vegetation cover factor (C): *C* factor was calculated using *NDVI* from remote sensing data with the application of the [Vander Knijff *et al*., 1999] equation. *NDVI* and *C* factor maps are shown in Figure-5. The distribution of *NDVI* (Figure-5.a) shows spatiotemporal changes. The average value of *NDVI* is 0.36, 0.41 and 0.43 for 2001-2002, 2013-2014 and2019-2020, respectively. For the classification of *NDVI*, we were based on the threshold used in Mohajane et al., 2018[40]. We attribute the class (-1; 0) to water; the class (0; 0.2) is attributed to low-density vegetation, the class (0.2; 0.5) is moderate-density vegetation and finally (0.5; 1)were given to high density vegetation. Moderate density vegetation is the most dominant class with 61.45%, 70.67% and 67.86% for the three dates, respectively (Table-1). Areas with moderate density vegetation cover constitute the dominant class in the watershed region over all years, with the larger area (70.67%) in 2013-2014.

In general, *C* factor values range from 0 to around 1, and they indicate the contribution to soil erosion susceptibility. Values close to 0 indicate protected areas and values close to 1 characterize areas with low vegetation cover. The resulting maps (Figure-5.b) show changes in *C* factor values over time. Overall, the watershed land shows low values of *C* factor in 2001-2002 and high values in 2019-2020. The mean value is about 0.35 in 2001-2002, while it is reduced to 0.28 and 0.25 in 2013-2014 and 2019-2020 respectively. Relatively protected areas (C< 0.2) are located in the North-East and in parts of the south of the watershed corresponding to high altitudes with natural vegetation. These areas cover 32.55, 41.24, and 46.56% of the total area (Table-2) in 2001-2002, 2013-2014 and 2019-2020 respectively. Areas surrounding Oued El kharroub and its main tributaries especially to the west of the study area show the highest values of the C factor (0.4<C<0.6 and 0.6<C<0.8). They correspond to areas with very low vegetation cover, cultivated land or bare land. They dominate the watershed area with a cumulative area percent of 41.4, 29.1 and 19.77 in 2001-2002, 2013-2014 and 2019-2020 respectively. Values those are greater than 0.8 occur in the waterbody of the dam.

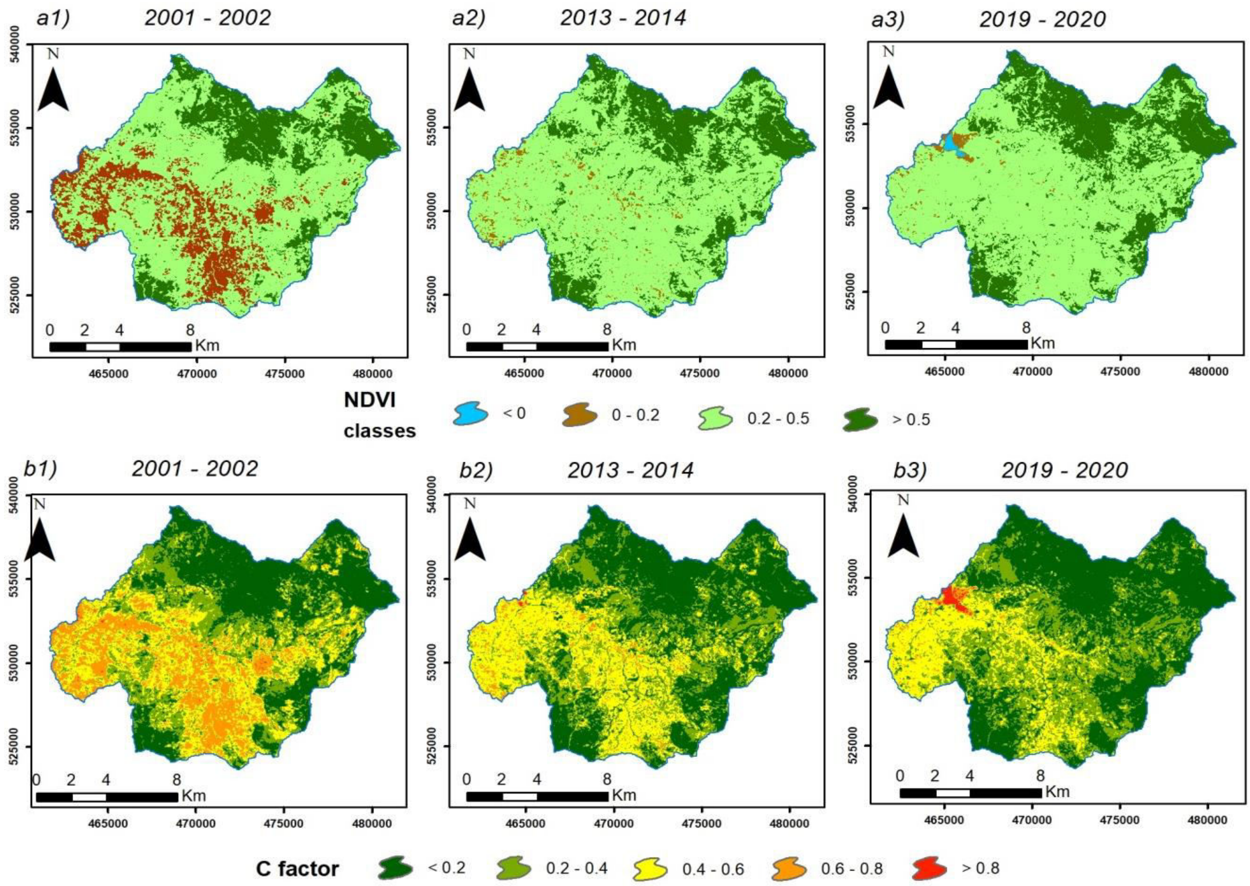

Figure-5. Distribution of *NDVI* (a1, a2, a3) and *C* factor (b1, b2, b3).

ARPN Journal of Engineering and Applied Sciences

Table-1. Variation of *NDVI* classes percent.

NDVI class	2001-2002		2013-2014		2019-2020	
	Area (km²)	%	Area (km²)	%	Area (km²)	%
NDVI < 0	0.13	0.07	0.13	0.07	0.76	0.42
0 <NDVI< 0.2	31.10	17.08	4.99	2.74	2.64	1.45
0.2 <NDVI< 0.5	111.91	61.45	128.69	70.67	123.58	67.86
NDVI > 0.5	38.96	21.39	48.29	26.52	55.13	30.27

Table-2. Variation of *C* factor classes' percent for the baseline period.

C factor class	2001-2002		2013-2014		2019-2020	
	Area (Km²)	%	Area (Km²)	%	Area (Km²)	%
< 0.2	59.27	32.55	75.10	41.24	84.78	46.56
0.2<*C*<0.4	47.03	25.83	53.83	29.56	60.08	32.99
0.4<*C*<0.6	43.01	23.62	47.23	25.94	33.53	18.41
0.6<*C*<0.8	32.41	17.80	5.68	3.12	2.47	1.36
> 0.8	0.38	0.21	0.26	0.14	1.24	0.68

P factor: In this region, the anti-erosion and crop management techniques are absent, so a value of 1 was given for the entire area of the watershed.

3.2 Assessment of Soil Erosion Rate Changes

The resulting thematic maps (Figure-6) show the spatial distribution of the erosion potential in t/ha/year under different scenarios. Estimated annual erosion rates are ranging from 0.47 to 1284.7 for the baseline period, from 0.37 to 1007.6 for 2021-2030 and from 0.36 to 1012.6for 2031-2050.Over the baseline period, there was a decreasing trend in erosion risk from 2000 to 2020, where average soil loss is 152.1, 86.8 and 37.9 for 2001-2002, 2013-2014 and 2019-2020, respectively. According to the projected model, soil losses may decrease to an average of 109.5 and 108.9 t/ha/year for 2021-2030 and 2031-2050 scenarios, respectively. This is could be explained by the changes in precipitations expected by the model.

In the entire watershed area, the most vulnerable areas are located in the middle, southern and western parts. These sites are characterized by soils sensible to erosion (K value =0.41) with low density vegetation cover (as highlighted by *NDVI* maps). In addition to these two factors, rainfall acts by its impact in promoting soil erosion. Some sites in the east region of the watershed are also known by high risk of erosion due to their high slope length and steepness. The erosion risk rates were classified into five classes: low erosion risk (A<7t/ha/year), medium erosion risk (7<A<20 t/ha/year), high erosion risk (20<A<70 t/ha/year), very high erosion risk (70<A<120 t/ha/year) and excessive risk (A>120 t/ha/year). For each class, the area and percentage were calculated (table. 3) for a simpler visualization of the erosion evolution. The most area of the watershed was attacked by very high to excessive soil erosion representing a cumulative percent of 66.61%, 57.59% and 57.45% for the baseline period, 2021-2030 and 2031-2050 scenarios respectively.

VOL. 18, NO. 6, MARCH 2023 ISSN 1819-6608
ARPN Journal of Engineering and Applied Sciences

www.arpnjournals.com

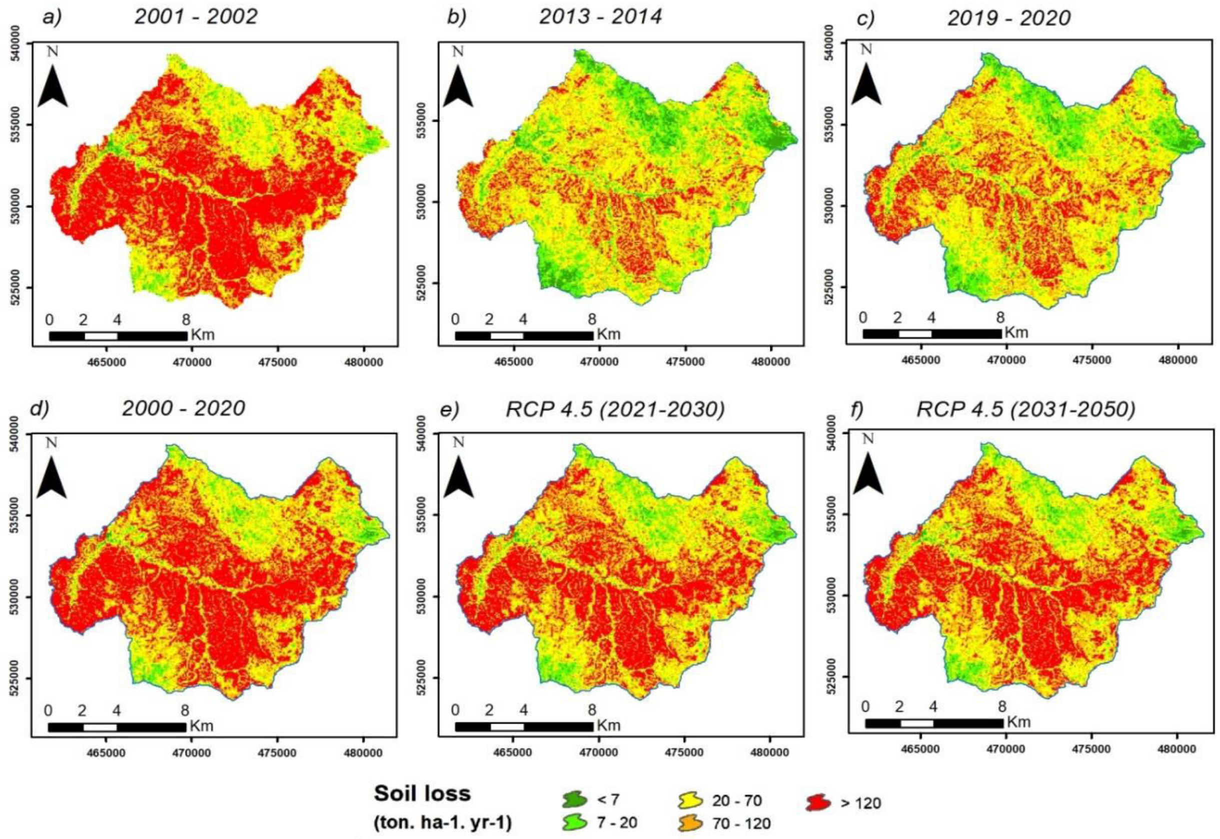

Figure-6. Spatial distribution of Soil loss for all scenarios.

Table-3. Variation of Soil loss classes' percent for allscenarios.

Scenario	Baseline (2000-2020)		RCP 4.5 (2021-2030)		RCP 4.5 (2031-2050)	
Soil loss class (t/ha/year)	Area in km²	Area in %	Area in km²	Area in %	Area in km²	Area in %
< 7	1.95	1.07	3.03	1.66	3.03	1.67
7 to 20	10.08	5.55	14.69	8.08	14.78	8.13
20 to 70	48.67	26.77	59.38	32.66	59.56	32.76
70 to 120	39.06	21.48	41.79	22.98	41.89	23.04
> 120	82.04	45.13	62.92	34.61	62.56	34.41

3.3 DISCUSSIONS

In this study, we highlighted precipitations and vegetation cover impact on soil erosion in the El kharroub watershed, suffering from agriculture activities. The mean soil loss found using the RUSLE model for the different scenarios: baseline period, RCP 4.5 (2021-2030) and RCP 4.5 (2031-2050) was 139.2, 109.5and 108.9 t/ha/year respectively. These values take place within the range(0 to 258.19t/ha/year) of erosion assessments done in the country scale by Gourfi *et al.*, 2018 [8] using the same model. However, they are high than the mean soil loss in Morocco which estimated to 5.06 t/ha/year. This comparison gives an indication that our study area falls into the regions the riskiest to erosion. Considering other studies in the Rif, we find that the risk of erosion in this watershed is higher where soil loss ranges from 0.3 to 819.43t/ha/year compared to the results found in Loukkos watershed [33] where soil erosion is varying from 0 to 362.2 t/ha/year for the baseline period 1981-2017, the watershed of Arbaa Ayacha [31] where soil loss was indicated between 0.11 and 468 t/ha/year and Tahaddart watershed [32] where values ranging from 0 to 202.3t/ha/year.

For the baseline period, the mean of *R* factor has decreased by 34.3% and the mean of *C* factor has decreased by 28.6% from 2002 to 2020, as a result, the mean of soil losses has decreased by 54.83%.Changes in amounts and intensities of precipitations are beyond the human being action, but natural vegetation can be controlled and increased. In our case study, there was a decreasing of *C* factor through reforestation taken by the regional direction of water and forests and the fight against desertification of the Rif, in order to protect soil and water resources in the watershed. The other factors have also significant effect on soil erosion risk distribution. The land is known by vulnerable soils that are easily detachable when are not protected by dense vegetation cover. The elevation of El kharroub watershed is varying from 41 to 1057m and steep slope (more than 15°) is represented by 21.39% of the total area. Also, the LS factor shows values from 0.1 to 37.1, this means that the length of the slope is short. This will affect soil detachment and mobilization but sediments will not be transported to long distances.

Against this backdrop, adopting on-site soil conservation practices is recommended. For example, the study adopted by Gong *et al.,* 2022 [41] showed that comparing with monocultures, mixed forests significantly reduced sediment yield by 23.6%. Related to slope steepness, the authors showed that this effectiveness was significant in areas with slope between 16 and 25°. However, in agricultural areas that are privatetofarmers, other soil conservation measures can be taken. For example, early planting of crops is better than later planting. The study of Le *et al.,* 2022[42]showed that early planting of cassavawas advantageous for decreasing soil loss through development of soil surface coverage and decreasing surface runoff. In addition, terraced cultivation technique in steep lands is beneficial for reducing runoff velocity as revealed by Meliho *et al.*, 2019 [13] in the Ourikawatershed in high Atlas of Morocco.

4. CONCLUSIONS

Despite the Rif is the first region threatened by water erosion risk in Morocco and its depending problems especially siltation of dams, a lot of watersheds feeding recently built dams have not ever been considered in environmental risk studies. El kharroub watershed is one of the areas falling into lack of academic literature. Our work is the first assessment of erosion vulnerability under present vegetation cover changes and present and future climate conditions in this watershed. The study showed that climate changes and vegetation cover are the main factors controlling erosion in this area. Therefore, attention should be taken to protect soils from non-expected high intensity precipitations and vegetation remediation needs to be encouraged. To conclude, for conserving soil and water resources in our watershed, reforestation has already practiced. However, other conservation measurements can be considered depending on the site characteristics.

ACKNOWLEDGMENTS

The authors would like to thank the Thematic Project 4 on Integrated Water Resources Management of the Institutional University Cooperation Program (CUI, VLIR-UOS) for the equipment used in this study. Thanks are also due to the anonymous reviewers for their valuable comments on this paper, which allowed us to improve the scientific quality of this research.

REFERENCES

[1] J. Ananda, G. Herath. 2003. Soil erosion in developing countries : A socio-economic appraisal. Journal of Environmental Management, 68 343-353. https://doi.org/10.1016/S0301-4797(03)00082-3.

[2] C. Qin, Z. Tanga, J. Chena, X. Chen. 2020. The impact of soil and water resource conservation on agricultural production- an analysis of the agricultural production performance in Zhejiang, China. Agricultural Water Management, 240, 106268. https://doi.org/10.1016/j.agwat.2020.106268.

[3] FAO. 2015. Food and Agriculture Organization of the Unated Nations. FAO Soils Portal. https://www.fao.org/soils-portal/about/en/.

[4] T. Gomiero. 2016. Soil Degradation, Land Scarcity and Food Security: Reviewing a Complex Challenge. Sustainability, 8(3): 281. https://doi.org/10.3390/su8030281.

[5] B. G. Sinshaw, A. M. Belete, Be. M. Mekonen, T. G. Wubetu,T. L. Anley, W. D. Alamneh, H. B. Atinkut, A. A. Gelaye, T. Bilkew, A. K. Tefera, A. B. Dessie, H. M. Fenta, A. M. Beyene, B. B. Bizuneh, H. T. Alem, D. G. Eshete, S. B. Atanaw, M. A. Tebkew, M. M. Birhanu. 2021. Watershed-based soil erosion and sediment yield modeling in the Rib watershed of the Upper Blue Nile Basin, Ethiopia. Energy Nexus, 3, 100023. https://doi.org/10.1016/j.nexus.2021.100023.

[6] Z. Gu, Y. Xie, Y. Gao, X. Ren, C. Cheng and S. Wang. 2018. Quantitative assessment of soil productivity and predicted impacts of water erosion in the black soil region of northeastern China. Science of the Total Environment, 637-638, 706-16. https://doi.org/10.1016/j.scitotenv.2018.05.061.

[7] A. Ahmed Khan, B. Ali Syeda. 2003. Effects of erosion on Indus river biodiversity in Pakistan. Pakistan journal of biological sciences. 6(12): 1035-1040.

[8] A. Gourfi, L. Daoudi, Z. Shi. 2018. The assessment of soil erosion risk, sediment yield and their controlling factors on a large scale: Example of Morocco. Journal of African Earth Sciences, 147, 281-299. https://doi.org/10.1016/j.jafrearsci.2018.06.028.

[9] M. Zare, A. Akbar, N. Samani, and M. Mohammady. 2016. Simulation of soil erosion under the influence of climate change scenarios. Environmental Earth

Sciences, 75: 1405. https://doi.org/10.1007/s12665-016-6180-6.

[10] M. A. Nearing, V. Jetten, C. Baffaut, O. Cerdan, and A. Couturier. 2005. Modeling response of soil erosion and runoff to changes in precipitation and cover. Catena, 61, 131-54. https://doi.org/10.1016/j.catena.2005.03.007.

[11] M. C. Passos Wichert, C. A. Alvares, J. C. Arthur Junior and J. L. Stape. 2018. Site preparation, initial growth and soil erosion in Eucalyptus grandis plantations on steep terrain. Forest sciences, 46, 17-30. DOI: dx.doi.org/10.18671/scifor.v46n117.02.

[12] Y. Guo, C. Penga,Q. Zhua, M. Wangc, H. Wangd, S. Penge,H. He. 2019. Modelling the impacts of climate and land use changes on soil water erosion: Model applications, limitations and future challenges. Journal of Environmental Management, 250, 109403. https://doi.org/10.1016/j.jenvman.2019.109403.

[13] C. Li, Z. Wang, Z. Li and X. Xu. 2021. Soil erosion impacts on nutrient deposition in a typical karst watershed. Agriculture, Ecosystems and Environment 322, 107649. https://doi.org/10.1016/j.agee.2021.107649.

[14] P. Porto, G. Callegari. 2021. Using ^{137}Cs measurements to estimate soil erosion rates in forest stands affected by wildfires. Results from plot experiments. Applied Radiation and Isotopes, 172, 109668. https://doi.org/10.1016/j.apradiso.2021.109668.

[15] Y. Li, Z. Wang, J. Zhao, Y. Lin, G. Tang, Z. Tao, Q. Gao, A. Chen. 2021. Characterizing soil losses in China using data of ^{137}Cs inventories and erosion plots. Catena 203, 105296. https://doi.org/10.1016/j.catena.2021.105296.

[16] M. Moukhchane. 2001. Différentes Méthodes d'estimation de l'érosion Dans Le Bassin Versant Du Nakhla (Rif Occidental, Maroc). Bulletin Réseau-Erosion. 21(39): 255-66.

[17] D. Gwapedza, N. Nyamela, D. A. Hughes, A. R. Slaughter, S. K. Mantel, B. v. d. Waal. 2021. Prediction of sediment yield of the Inxu River catchment (South Africa) using the MUSLE. International Soil and Water Conservation Research, 9, 37-48. https://doi.org/10.1016/j.iswcr.2020.10.003.

[18] M. Boufala, A. El Hmaidi, K. Chadli, A. Essahlaoui, A. El Ouali, S. Taia. 2019. Hydrological modeling of water and soil resources in the basin upstream of the Allal El Fassi dam (Upper Sebou Watershed , Morocco). Modeling Earth Systems and Environment. https://doi.org/10.1007/s40808-019-00621-y.

[19] R. K. Bhattacharya, D. C. Nilanjana, D. Kousik. 2020. Sub-basin prioritization for assessment of soil erosion susceptibility in Kangsabati, a plateau basin : A comparison between MCDM and SWAT models. Science of the Total Environment, 734, 139474. https://doi.org/10.1016/j.scitotenv.2020.139474.

[20] B.F. Admas, T. Gashaw, A.A. Adem, A. W. Worqlul, Y. T. Dile and E. Molla. 2022. Identification of soil erosion hot-spot areas for prioritization of conservation measures using the SWAT model in Ribb watershed, Ethiopia. Resources, Environment and Sustainability, 100059. https://doi.org/10.1016/j.resenv.2022.100059.

[21] W.H. Wischmeier, D.D. Smith. 1978. Predicting Rainfall Erosion Losses: A Guide to Conservation Planning. Handbook. Department of Agriculture, Washington, D.C. p. 537.

[22] G. Singh, R. K. Panda. 2017. Grid-cell based assessment of soil erosion potential for identification of critical erosion prone areas using USLE, GIS and remote sensing: A case study in the Kapgari watershed, India Gurjeet. International Soil and Water Conservation Research, 5(3): 202-11. https://doi.org/10.1016/j.iswcr.2017.05.006.

[23] T. Gia Pham, J. Degener, M.Kappas. 2018. Integrated universal soil loss equation (USLE) and Geographical Information System (GIS) for soil erosion estimation in A Sap basin: Central Vietnam. International Soil and Water Conservation Research, 6 (2): 99-110. https://doi.org/10.1016/j.iswcr.2018.01.001.

[24] K.G. Renard, G.R. Foster, G.A. Weesies and J.P. Porter. 1991. RUSLE: Revised Universal Soil Loss Equation. Journal of Soil and Water Conservation. 46, 30-33.

[25] P. Borrelli, *et al*. 2021. Soil erosion modelling : A global review and statistical analysis. Science of the Total Environment, 780, 146494. https://doi.org/10.1016/j.scitotenv.2021.146494.

[26] P. Chuenchum, M. Xu, W. Tang. 2020. Predicted trends of soil erosion and sediment yield from future land use and climate change scenarios in the Lancange-Mekong River by using the modified RUSLE model. International Soil and Water Conservation Research, 8 (3): 213-27. https://doi.org/10.1016/j.iswcr.2020.06.006.

[27] S. N. Mhaske, K. Pathak, S. Sandeep, and D. Bikas. 2021. Assessment and management of soil erosion in the hilltop mining dominated catchment using GIS integrated RUSLE model. Journal of Environmental Management, 294, 112987. https://doi.org/10.1016/j.jenvman.2021.112987.

[28] J. Wang, P. Lu, D. Valente, I. Petrosillo, S. Babu, S. Xu, C. Li , D. Huang, M. Liu. 2022. Analysis of soil erosion characteristics in small watershed of the loess tableland Plateau of China. Ecological Indicators, 137, 108765. https://doi.org/10.1016/j.ecolind.2022.108765.

[29] Y. S. Kebede, N. T. Endalamaw, B. G. Sinshaw, H. B. Atinkut. 2021. Modeling Soil Erosion Using RUSLE and GIS at Watershed Level in the Upper Beles, Ethiopia. Environmental Challenges, 2, 100009. https://doi.org/10.1016/j.envc.2020.100009.

[30] N. Aouichaty, Y. Bouslihim, S. Hilali, and A. Zouhri. 2022. Estimation of water erosion in abandoned quarries sites using the combination of RUSLE model and geostatistical method. Scientific African, 16, e01153. https://doi.org/10.1016/j.sciaf.2022.e01153.

[31] A. Ouallali, M. Moukhchane, H. Aassoumi, F. Berrad and I. Dakir. 2016. Evaluation et cartographie des taux d'érosion hydrique dans le bassin versant de l'Oued Arbaa Ayacha (Rif occidental, Nord Maroc). Bull. l'Institut Sci. Rabat, Sect. Sci. la Terre. 38(2458-7184): 65-79.

[32] M. Tahiri, H. Tabyaoui, F. El hammichi, M. Achab, A. Tahiri, H. El hadi. 2017. Quantification of Water Erosion and Sedimentation Using Empirical Models in the Tahaddart Watershed (Northwestern Rif, Morocco). Bulletin de l'Institut Scientifique, 39, 87–101.

[33] S. Acharki, F. El, Y. Arjdal, M. Amharref, A. Samed, and H. Ben. 2022. Soil erosion assessment in northwestern Morocco. Remote Sensing Applications: Society and Environment, 25, 100663. https://doi.org/10.1016/j.rsase.2021.100663.

[34] A. Alitane, A. Essahlaoui, M. El Hafyani, A. El Hmaidi, A. Kassou, Y. El Yousfi, A. Griensven, C. J. Chawandaand A. V. Rompaey. 2022. Water erosion monitoring and prediction in response to the effects of climate change using RUSLE and SWAT equations: case of R'Dom watershed in Morocco. Land, 11, 93. https://doi.org/10.3390/land11010093.

[35] P. Marcinkowski, S. Szporak-wasilewska, I. Kardel. 2022. Assessment of soil erosion under long-term projections of climate change in Poland. Journal of Hydrology, 607, 127468. https://doi.org/10.1016/j.jhydrol.2022.127468.

[36] G J Wall, D R Coote, E.A. Pringle, I.J. Shelton. 2002. RUSLE-CAN – Équation Universelle Révisée Des Pertes de Sol Pour Application Au Canada. Ottawa (Ontario).

[37] K.G. Renard, J.R. Freimund. 1994. Using Monthly Precipitation Data to Estimate the R Factor in the Revised USLE. Journal of Hydrology, 157, 287-306. http://dx.doi.org/10.1016/0022-1694(94)90110-4.

[38] H. Mitasova and L. R. Iverson. 1996. Modelling topographic potential for erosion and deposition using GIS. International Journal of Geographical Information Systems, 10(5), 629-641. DOI: 10.1080/02693799608902101.

[39] J. Van der Knijff, R. Jones, L. Montanarella, 2000. Soil erosion risk assessment in Europe. EUR 19044 EN. Luxembourg.

[40] M. Mohajane, A. Essahlaoui, F. Oudija, M. El Hafyani, A. El Hmaidi, A. El Ouali, G. Randazzoand, A C. Teodoro. 2018. Land Use/Land Cover (LULC) Using Landsat Data Series (MSS, TM, ETM+ and OLI) in Azrou Forest, in the Central Middle Atlas of Morocco.Environments, 5, 131. doi:10.3390/environments5120131.

[41] C. Gong, Q. Tan, G. Liu and M. Xu. 2022. Impacts of mixed forests on controlling soil erosion in China. Catena, 213, 106147. https://doi.org/10.1016/j.catena.2022.106147.

[42] H. Le, M. Shibata, Y. Kohmoto, L. Nguyen and S. Funakawa. 2022. Analysis of the processes that generate surface runoff and soil erosion using a short-term water budget on a mountainous sloping cropland in central Vietnam. Catena, 211, 106032. https://doi.org/10.1016/j.catena.2022.106032.